

A MISSION ASSESSMENT OF AERO ENGINE LOSSES

Oskar Thulin
Chalmers University of Technology
SE-412 96 Göteborg, Sweden
oskar.thulin@chalmers.se

Jean-Michel Rogero
Airbus Operations S.A.S.
31060 Toulouse Cedex 09, France

Tomas Grönstedt
Chalmers University of Technology
SE-412 96 Göteborg, Sweden

Abstract

A detailed and systematic loss breakdown of a direct drive two-spool turbofan aero engine integrated to an aircraft corresponding to a technology level of year 2020 is produced from engine mission point performance simulations. The analysis includes the fundamental mission points throughout a commercial aircraft mission. The breakdown also incorporates the inherent effects of the propulsion system such as engine weight and nacelle drag. A new term, installed rational efficiency, is proposed to fully assess the performance of the propulsion subsystem. Combining the detailed component loss analysis with the assessment of the installation effects provides a systematic as well as effective way of analyzing the full impact of an aircraft component, like the engine subsystem, on the aircraft. This can be used to truly assess the performance of one propulsion unit compared to another.

Nomenclature

A Area
C Absolute velocity
F Thrust
L/D Lift over drag coefficient
i Irreversibility rate
*i** Normalized irreversibility rate
Ma Mach number
P Power
Q Heat transfer
R Gas constant

T Temperature
U Flight velocity
V Relative velocity
a Acceleration
c_x Thrust coefficient
g Gravitational constant
h Specific enthalpy
m Mass flow
p Pressure
s Specific entropy
x Mole fractions
 ψ Rational efficiency
 α Angle of attack
 β Mass proportion of constituent in fuel
 δ Deviation angle between aircraft direction and engine direction
 ϵ Specific exergy
 γ Path angle
 λ Mass fraction of constituent per unit of post combustion fluid
 η Polytropic efficiency

Subscripts

Booster Intermediate pressure compressor
Brn Burner
D Drag
DBP Bypass Duct
FanBP Fan Bypass section
HPC High pressure compressor
HPT High pressure turbine
ICD Inter Compressor duct
Intake Engine intake
ITD Inter turbine duct
JetP Core nozzle duct
(incl. Turbine Rear Structure)
L Lift
LPT Low pressure turbine
RBP Reintroduction of surge avoidance bleed in Bypass duct

s	Shaft
T	Thrust
W	Weight
bld	Bleed
cabin	Cabin
eng	Engine
f	Fuel, Formation
i	Iteration variable
in	Into control volume
out	Out of control volume
sf	Standard formula
ss	Standard state
syst	System level
∞	Ambient condition
30	High pressure compressor exit (total)
40	High pressure turbine entry (total)

Surprisingly, exergy based methods still seem to be in limited use for analysis of aero gas-turbine engines. Having said this, it should be noted that monitoring and analysing entropy production is a common method for aero engine turbomachinery component analysis. The entropy production term, is directly related to the exergy destruction through the multiplication with a reference temperature. The use of entropy production in analysis of turbomachinery can hence be seen as nothing but an implicit use of the exergy methodology. However, for aero engine systems the situation still seems to be that exergy analysis is in limited use.

Introduction

Reducing engine losses is of paramount importance in the aerospace industry. Using the conventional method to estimate irreversibility, different losses are typically accounted for using turbomachinery efficiencies, pressure loss coefficients, mechanical efficiencies and mixing losses. To fully comprehend how the different engine parameters may affect the overall performance requires extensive experience and trade-offs are made using parameters of different impact, e.g. compressor efficiency, nacelle drag and engine weight. Propulsion concept development, selection and integration is truly one of the most complex challenges in an aircraft, it constitutes a highly multidimensional and tightly coupled system.

Today, parametric studies on a baseline model are typically used to estimate the effect of incremental improvements to the engine. This method does not allow for a way to make the losses comprehensible, only to study the effect of a change. Methods exist, based on exergy analysis, that are able to assess the component contribution to the overall losses and relate the losses to each other in a unified framework.

Using the exergy methodology allows analysis of the engine performance in one common currency, that fully takes advantage of the possibilities in the first and second law of thermodynamics. Exergy calculations relate the thermodynamical properties of a fluid stream to an equilibrium state to determine the work potential at each station in the engine. The further away the thermodynamical properties are from the equilibrium state, the larger the work potential is. Tracking the loss of work potential in each component throughout the cycle clearly indicates where the irreversibilities occur.

Horlock and Clark pioneered the field of exergy analysis by applying it to a turbojet as early as 1975 [1]. Their original work was derived from extending the work of Evans [2]. In 1995, Brilliant extended the analysis for a turbofan engine [3] which was studied at the cruise point. Roth and Mavris wrote a series of papers on the subject, especially interesting for the scope of this work is a full mission study of a military fighter aircraft from 2000 [4]. Grönstedt et al. used exergy analysis in the cruise point to evaluate different future commercial engine concepts

including a turbofan 2050 reference, a pulse detonation combustion engine and an open rotor engine [5]. Zhao et al. continued the exploration of exergy analysis by applying it to better understand the benefits of intercooling in turbofan aero engines [6].

Rosen previously took a small step in the direction of providing a commercial engine mission study but the analysis failed to provide understanding of the loss sources throughout a commercial aircraft mission [7]. Rosen assumed engine performance data and flight conditions which are far from typical airline operation. This paper provides a breakdown of the irreversibilities during the different main points that constitute a full mission of a commercial aircraft engine. A modern direct-drive two-spool turbofan engine was chosen as the engine architecture in this study, due to its dominating market share.

This paper will not only provide a detailed study of a multi-operating point turbofan but also aims at extending the concept of exergy from the analysis of pure thermodynamic effects to include the consequences of the implementation on the aircraft to the overall mission energy requirements and hence be able to fully compare different implementation integrated at vehicle level. Paulus and Gaggioli wrote a simple but inspiring contribution presenting the exergy associated with lift [8]. The analysis in this paper includes weight from the engine and the pylon, as well as drag caused by the nacelle. The analysis also includes engine bleed and power extraction. Including the installation effects will give a direct comparison between the engine aerodynamic properties and mass associated with the engine. A new term, *installed rational efficiency* is proposed, making it possible to compare the complete impact on the

aircraft for one propulsion unit with another.

Aero Engine Exergy Theory

The most significant energy fluxes in an aero component are thrust, mechanical work, kinetic energy, thermomechanical energy and chemical energy. These fluxes are therefore included in the aero engine exergy analysis presented here. The formulation is based on the work of Horlock and Clark [1]. Horlock and Clark provided the analysis for the assumption of perfect gas. However, in this paper the treatment has been adopted to real gases to be used in state of the art engine performance codes.

The maximum work that can be obtained for an aero engine system is given by

$$\left(\sum_i \dot{m}_i \varepsilon_i \right)_{in} \geq P_S + P_T - \sum_i \int \frac{T - T_\infty}{T} dQ_i + \left(\sum_i \dot{m}_i \varepsilon_i \right)_{out} \quad (1)$$

and is illustrated in Fig.1. The maximum work is obtained in reversible limit at which equality holds [9]. The equation corresponds to the exergy balance of the incoming and outgoing exergy fluxes and is a measure of the irreversibility of the system.

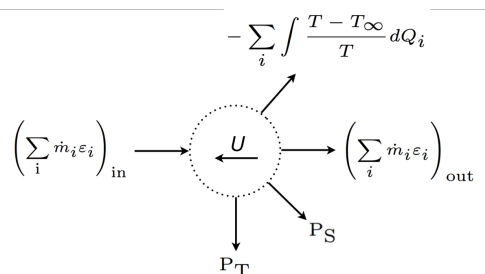


Figure 1: Second law of thermodynamics applied to the reference frame of the engine

The irreversibility rate, also called the exergy destruction i , is formed as a difference when bookkeeping the exergy crossing the boundaries of a control volume:

$$i = \left(\sum_i \dot{m}_i \varepsilon_i \right)_{\text{in}} - \left(\sum_i \dot{m}_i \varepsilon_i \right)_{\text{out}} - P_S - P_T + \sum_i \int \frac{T - T_\infty}{T} dQ_i. \quad (2)$$

When the reference environment is set to the ambient conditions, the total magnitude of exergy that enters into the system is equal to the exergy of the fuel. Relating the component irreversibilities to the total exergy gives the ratio of irreversibility for each component, then

$$i^* = \frac{i}{\dot{m}_f \varepsilon_f}. \quad (3)$$

Adding up all the irreversibility contributions give a ratio of the total irreversibility

$$i_{\text{sys}}^* = \frac{\sum_i i_i}{\dot{m}_f \varepsilon_f}. \quad (4)$$

The rational efficiency expresses the useful work of a control volume in relation to the incoming exergy flux. The useful power generated by the aero engine is the thrust it provides to the aircraft as well as the bleed and power it potentially supplies to the cabin. Cabin bleed and power are not commonly included in the rational efficiency term. However, it is useful work delivered to the aircraft and hence it ought to contribute to the useful work term. Thus we define

$$\Psi_{\text{sys}} = \frac{\sum_i P_{T,i} + [(\dot{m}\varepsilon)_{\text{bld}} + P_s]_{\text{cabin}}}{\dot{m}_f \varepsilon_f}. \quad (5)$$

The different terms in Eq.1 are described in more depth in the Appendix.

Installed rational efficiency

The net thrust generated by the engine is propelling the aircraft. A part of this thrust is compensating for the fact that the engine sub system adds weight and engine external

drag to the aircraft. This paper presents a method to account for these losses of useful power, to truly assess the full impact of the engine subsystem towards the aircraft. The principle of accounting for engine components as the weight and potential drag that need to be compensated for can be extended to include every aircraft component in order to truly assess the full performance of the aircraft in a systematic way. The authors have chosen to apply the method to the engine and its installation to give the engine community a way to assess the full engine performance.

The external drag is easily compensated for by multiplying the object's velocity with the thrust that is required to balance the drag force, namely

$$P_{T,\text{drag}} = U \frac{F_{\text{drag}}}{\cos(\alpha - \delta)}. \quad (6)$$

Compensating for weight is slightly more complicated. Using a known lift over drag ratio provides a way to accomplish this. Combining the force balances of an aircraft in the directions of parallel to as well as perpendicular to the flight trajectory, gives the equation that is necessary to evaluate how much thrust is required to carry a certain weight. This equation, as opposed to the drag, can be divided into two parts: 1) a dissipating and a 2) non-dissipating and hence exergy accumulating part. The steady state contribution of the non-dissipative part is accumulated as potential power in climb and can later on be harvested in descent. The acceleration terms will add to the momentum and are by definition non-dissipative. The term corresponding to the misalignment of thrust to the aircraft trajectory, $\cos(\alpha - \delta)$, contributes to the dissipative part when different from one. The product when multiplying the thrust equation with the object's velocity is equivalent to the magnitude of

the useful power that is consumed in order to carry a certain weight. The equation with the different parts denoted explicitly becomes:

$$P_{T,weight} = U \frac{m_{eng}}{\cos(\alpha - \delta)} \left(\underbrace{a_D + \frac{1}{L/D} a_L}_{\text{Acceleration}} + \underbrace{g \sin(\gamma)}_{\text{Potential}} + \underbrace{\frac{1}{L/D} g \cos(\gamma)}_{\text{Dissipative}} \right). \quad (7)$$

Using the drag- and the weight-thrust equation, i.e. Eq.6 and Eq.7 respectively, along with the ordinary engine component loss breakdown makes it possible to assess the impact of all different engine related subsystems towards the aircraft.

Here a new term called *installed rational efficiency* is introduced, to take the deduction of power needed to compensate for the weight and drag associated with the engine subsystem. In descent, the harvested potential exergy adds, along with the fuel exergy, to the incoming exergy flux. In climb, the stored potential exergy is seen as stored within the control volume and thereby not yet consumed. Including stored and harvested potential exergy in the numerator is also valid for the irreversibility equations in Eq.2 and Eq.3. For reasons previously outlined the bleed and power supplied to the airframe need to be included in numerator. The full equation becomes

$$\Psi_{\text{system,inst}} = \frac{\left[\sum_i P_{T,i} - (P_{T,eng-W} + P_{T,eng-D}) \right] + [(\dot{m}\epsilon)_{\text{bld}} + P_s]_{\text{cabin}}}{\left[\dot{m}_f \epsilon_f - P_{T,eng-W-\text{stored potential}} + P_{T,eng-W-\text{harvested potential}} \right]}. \quad (8)$$

It shall be noted that engine weight is not only a burden for the system since it also contributes to wing load alleviation. This is however a secondary effect which is complex to assess. Its influence has therefore been neglected in this paper.

Engine architecture and mission point specification

As an example to carry the analysis a generic aircraft equipped by two-spool generic engines was defined by Chalmers based on public information. The engine setup was designed in a multi point design process in PROOSIS® [10] to reflect a typical modern engine of a technology level corresponding to year 2020. Some important information about the PROOSIS® setup regarding exergy can be found in the Appendix. The engine performance can be seen in Tab.1.

The mission-point specification from an external aircraft model can be seen in Tab.2, where mid climb, top of climb, begin of cruise, end of cruise and descent are all included. A lift-over-drag coefficient as well as an angle that describes how the engine is lined up compared to the aircraft are both required for the installed exergy calculations. They are assumed to be 23 and 2.5 degrees, respectively. The lift-over-drag coefficient will in reality differ slightly over the different points. For simplicity reasons it has been chosen to be constant in frame of the analysis in this paper.

Engine performance modeling does not typically require design of engine internal component areas. However, knowledge about the component velocities is necessary when using the exergy methodology. Engine areas were designed to be corresponding to typical engine component Mach numbers in cruise. These Mach numbers, that can be found in Tab.3, were selected based on the work by Grieb [11], and extrapolated to year 2020 performance level.

To compensate for the engine subsystem weight and drag additional modeling was required. Nacelle drag was assessed for the different missions points by using a Chalmers in-house code based on the report

Table 1: Engine specifications for different mission points

	Mid Climb	Top of Climb	Begin of Cruise	End of Cruise	Descent
η_{FAN-BP}	0.93090	0.92900	0.93073	0.93078	0.48999
$\eta_{FAN-CORE\&BOOSTER}$	0.90472	0.89483	0.90417	0.90561	0.87688
η_{HPC}	0.90406	0.89397	0.90616	0.90856	0.86553
η_{HPT}	0.91116	0.91100	0.90897	0.90849	0.85016
η_{LPT}	0.91309	0.91068	0.90947	0.90933	0.88538
T_{30} (K)	838.99955	800.82353	774.07702	768.23483	553.35047
T_{41} (K)	1733.01201	1682.95751	1604.90967	1589.00544	1154.98451
OPR	41.65294	45.39788	41.68407	40.97466	9.27412
BPR	12.62240	12.34636	12.66769	12.73707	22.57642
FPR	1.47680	1.53658	1.48324	1.47292	1.03847
$\pi_{FAN-CORE\&BOOSTER}$	2.26981	2.37901	2.28933	2.27048	1.28911
\dot{W}_1 (kg/s)	311.16049	184.42970	181.68668	180.54454	180.40627
SFC (mg/Ns)	13.41601	14.45390	14.69187	14.71214	-167.61114

Table 2: Mission point Specification

	Mid Climb	Top of Climb	Begin of Cruise	End of Cruise	Descent
alt (ft)	20000	37000	37000	37000	20000
M	0.589	0.77	0.79	0.79	0.589
α (deg)	2.78	3.29	2.97	2.84	2.63
γ (deg)	2.79	0.54	0.00	0.00	-3.15
$F_N(N)$	37500	20500	18000	17500	-500
time after take-off (min)	8	25	25	95	105

Table 3: Engine component Mach numbers

$Ma_{Intake,out}$	0.603
$Ma_{Booster,out}$	0.422
$Ma_{ICD,out}$	0.482
$Ma_{HPC,out}$	0.263
$Ma_{Brn,out}$	0.150
$Ma_{HPT,out}$	0.420
$Ma_{ITD,out}$	0.368
$Ma_{LPT,out}$	0.322
$Ma_{JetP,out}$	0.322
$Ma_{FanBP,out}$	0.452
$Ma_{DBP,out}$	0.452
$Ma_{RBP,out}$	0.452

Exergy breakdown of the engine thermodynamic cycle

A breakdown of the total exergy is performed at each mission point to indicate what is useful, as seen from the control volume of the propulsion system. Aggregating the mission points that are presented in this paper as well as one take-off point into a total mission breakdown enables the possibility of showing the full mission engine performance. A mission total breakdown of what is useful for the engine can be found in Fig.2(a). The total was calculated by summing the products of the exergy flow per time unit with the time spent on each point during a regional aircraft mission. The fuel burn before take-off is neglected in this analysis. The aircraft was considered to land at the same altitude as it took off from. The thermodynamical reference used in the exergy calculations was changed along with the changing ambient condition at different altitudes since the

ESDU 81024 [12]. Engine sub system weight was modeled in an in-house developed conceptual design tool called WEICO [13]. The engine weight was estimated to 3280kg. The conceptual design of the engine included 3 booster stages, 10 HPC stages, 2 HPT stages and 7 LPT stages. Weight for pylon was also included in the analysis since it is a direct effect of having an engine mounted on the wing and ultimately attached to the aircraft. It was estimated to 492kg.

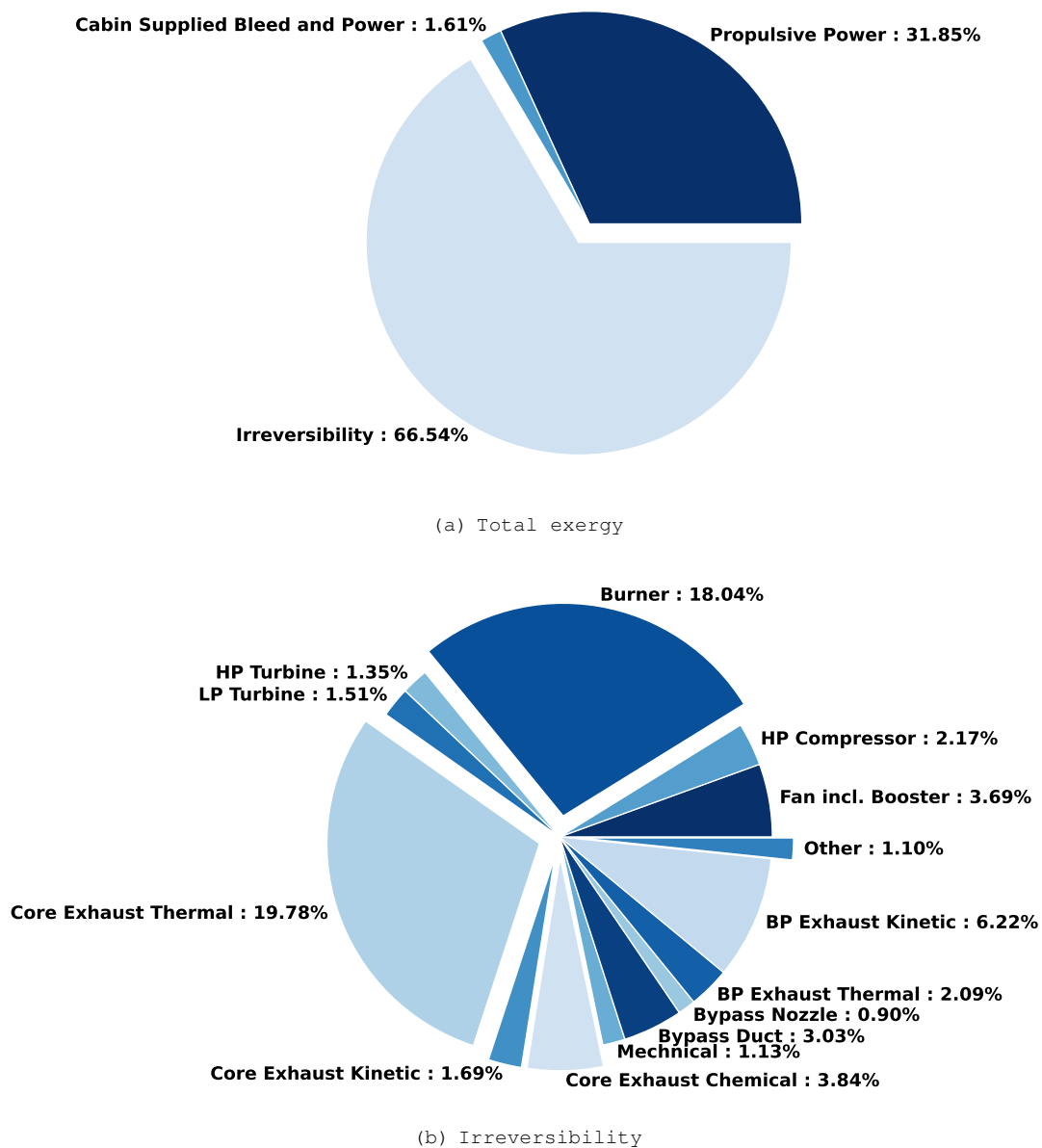


Figure 2: Mission Total - Breakdown.

Table 4: Results of the Total Breakdown of all mission points normalized with fuel exergy

	Mid Climb	Top of Climb	Begin of Cruise	End of Cruise	Descent
Propulsive Power	0.31433	0.35670	0.36009	0.35961	-0.02235
Cabin Supplied Bleed and Power	0.01250	0.01636	0.01795	0.01832	0.04513
Irreversibility	0.67317	0.62694	0.62196	0.62206	0.97722
Rational Efficiency	0.32683	0.37306	0.37804	0.37794	0.02278

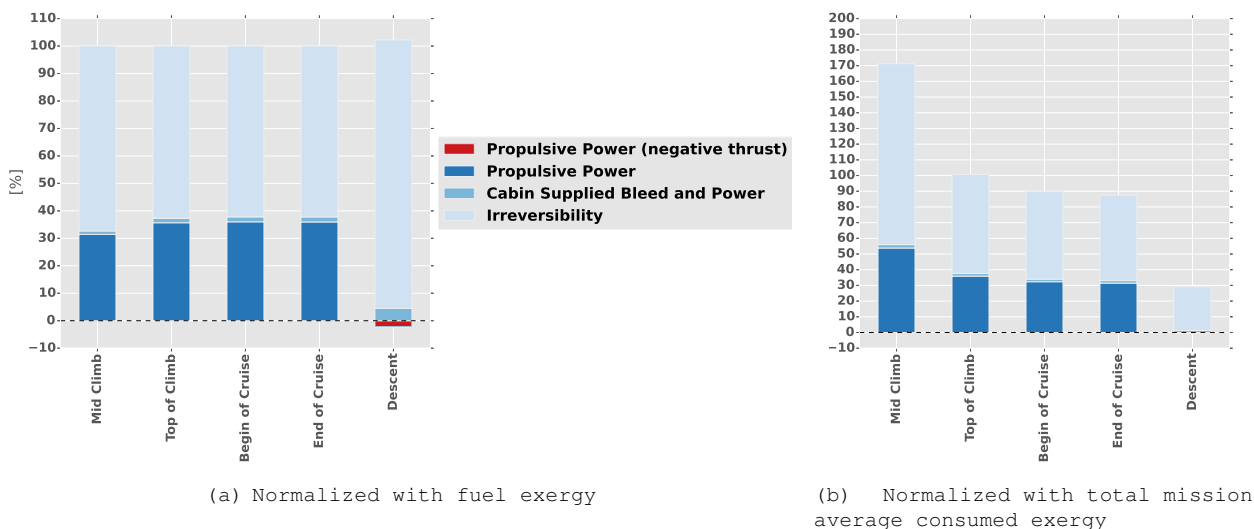


Figure 3: Mission point comparison - Exergy breakdown.

instantaneous ambient conditions is setting the instantaneous limit of the maximum work possible of a system during a process that brings the system to complete equilibrium its the surroundings.

Almost two thirds of the entered fuel exergy is corresponding to engine internal irreversibilities. The additional part is constituting the rational efficiency where the propulsive power is about twenty times as large as the cabin supplied bleed and power.

The simulated mission points that constituted the mission are presented independently in both Fig.3(a) and Tab.4. It can be noted that the higher loaded mid climb point which is further from design conditions have a lower rational efficiency than the lower loaded top of climb and cruise points. The descent point is simulated having a negative thrust, this causes the irreversibilities to be larger than the entered fuel exergy. Each point is normed with the fuel exergy that is consumed during the corresponding point. This shows how well the engine performs at a

specific point but does not provide a way to compare the losses between the points to each other.

In order to give the perspective of how the points compare to each other an additional stacked bar chart was created, as seen in Fig.3(b). This chart was not normed with the fuel exergy consumed at the point but instead the mission total average fuel exergy. The more highly loaded mid climb point consumed significantly more fuel which make the magnitude significantly larger than for the other points. The cruise points consume about 90% of the total mission average fuel exergy. The latter cruise point slightly less due to the lower lift requirement caused by the lower fuel weight. The large relative engine irreversibility in the descent point can be seen to be small in absolute numbers in comparison to the other points.

Irreversibility breakdown of the engine propulsion cycle

The analysis is also accompanied by a breakdown of all irreversibilities on component level. When summing up

the irreversibility percentages in the irreversibility breakdown, it equals the magnitude of the irreversibility in the total exergy breakdown.

A total mission irreversibility breakdown is presented in Fig.2(b). Looking at the different irreversibilities, some are more accessible to decrease than others. Work has previously been done on excluding the irreversibilities from the analysis that are considered to be impossible to lower. To assess what technology that cannot be invented would be highly unproductive in terms of looking for future engine concepts. As well as it would make comparison between different concepts problematic and understanding of how the losses truly distribute hard.

The total turbomachinery losses corresponds to 8.72 fuel exergy percentage units of which 40% originates from the turbomachinery located on the high pressure shaft. The turbomachinery losses are equivalent of a little bit more than 13% of the total engine irreversibility. Even though the turbomachinery related losses are small in comparison to the other irreversibilities, as being one of the major weight drivers in the engine it is important that high efficiency is achieved at lower component weight.

The burner contributes as one of the two major sources to the total irreversibility. This is despite that combustion efficiency is almost at one. The combustion irreversibilities is an inherent effect of constant pressure combustion used in turbofans. The large irreversibilities comes from the massive entropy production in combustion. In order to limit the entropy production, it would be beneficial to combust at a steeper curve in a temperature-entropy (TS) diagram. Constant volume combustion is a way to accomplish this since isochores on a TS diagram are steeper

than isobars.

The ducts have a very small contribution to the engine propulsion system irreversibilities, needless to say that well-designed ducts are however important for the performance of the other component as well as it is important for limited engine weight. The only exception to the statement about low irreversibilities in the ducts is the bypass duct which has a much larger contribution to the irreversibilities due to the large magnitude of mass flow that is passed through the duct. The bypass nozzle compared with the core nozzle show a similar effect that is also mainly caused by the large mass flow.

The mechanical efficiency is set to 99.8% for both shafts. A resulting irreversibility of 1.13% makes it clear that the large amount of power that is transferred via the shafts leads to much higher losses on a system level than what is indicated by the efficiency number by itself.

Unused exergy in the flow leaving the engine is included in the exhaust component. Note that all exhaust irreversibilities are broken down into the different exergy fluxes. The term corresponding to "thermomechanical" exergy is here named "thermal" since it better describes the specific exergy flow. The reasoning is that the pressure difference to ambient conditions will only contribute in the nozzle thrust term and not show up as an irreversibility.

Thermal exhaust irreversibilities is a result of that the flow is energized in the engine cycle and then not brought to thermal equilibrium with the ambient conditions. The thermal exhaust irreversibility is the largest contribution to the total irreversibilities, it causes nearly 30% of the engine cycle irreversibility. The exhaust flow for the core is in excess of 450 degrees

Table 5: Results of the Irreversibility Breakdown of all mission points normalized with fuel exergy

	Mid Climb	Top of Climb	Begin of Cruise	End of Cruise	Descent
Inlet	0.00501	0.00440	0.00486	0.00496	0.01744
Fan incl. Booster	0.03314	0.03337	0.03259	0.03258	0.13138
Intercompressor Duct	0.00147	0.00132	0.00143	0.00145	0.00267
Core leakage	0.00046	0.00051	0.00054	0.00054	0.00035
HP Compressor	0.02220	0.02251	0.02083	0.02049	0.03819
Burner Inlet Duct	0.00120	0.00107	0.00115	0.00117	0.00200
Burner	0.18433	0.15986	0.16776	0.16949	0.28672
HP Turbine	0.01302	0.01092	0.01219	0.01248	0.03579
Interturbine Duct	0.00072	0.00064	0.00069	0.00070	0.00119
LP Turbine	0.01484	0.01412	0.01524	0.01545	0.01672
Jet Pipe Duct	0.00073	0.00065	0.00070	0.00071	0.00120
Core Nozzle	0.00070	0.00102	0.00104	0.00103	0.00030
Core Exhaust Thermal	0.20108	0.19523	0.19110	0.19051	0.27044
Core Exhaust Kinetic	0.01726	0.02159	0.01540	0.01429	0.00661
Core Exhaust Chemical	0.03716	0.04036	0.03988	0.03978	0.03348
Mechanical	0.01141	0.01142	0.01153	0.01155	0.00803
Bypass Duct	0.02821	0.02475	0.02737	0.02794	0.10147
Booster Bleed into BP	0.00000	0.00000	0.00000	0.00000	0.00374
Bypass Nozzle	0.00738	0.00904	0.01023	0.01043	0.01652
BP Exhaust Thermal	0.00056	0.03525	0.03163	0.03026	0.00280
BP Exhaust Kinetic	0.09229	0.03890	0.03583	0.03625	0.00021
BP Exhaust Chemical	0.00000	0.00000	0.00000	0.00000	0.00000

kelvin warmer for the simulated engine than the ambient conditions in cruise. This temperature difference does not in itself contribute to the thrust at all and hence can be seen as a major term. The bypass thermal irreversibility is much lower since the only increase of enthalpy takes place in the bypass section of the fan.

The exhaust gases are more rich on H₂O and CO₂ than the gas composition found in the ambient air, these compositions have different exergy levels due to the different set of partial pressures. For the exhaust gas the exergy is higher. It could be theoretically possible to obtain work from gases with various partial pressures, but would be highly impractical in reality. One could see this loss as a direct result of that fuel is burned.

The last but not least term is the kinetic irreversibilities in the exhaust flows. All kinetic energy in the exhaust flow does not contribute to the thrust, the kinetic

irreversibility is corresponding to the portion of the kinetic energy that does not propel the aircraft. This term is hence directly related to the propulsive efficiency.

The outcome of the irreversibility distribution of the different mission points can be seen in Tab.5.

Radar charts were produced to illustrate how the irreversibilities changes comparing the different mission points. The largest loss sources can be found in Fig.4(a) and the corresponding sources normed with the mission total average fuel exergy is illustrated in Fig.4(b). The mid climb point does not choke in the bypass nozzle which explains the much lower thermal exhaust irreversibility, but on the other hand significantly higher kinetic exhaust irreversibility, compared to the top of climb and the cruise points. The other components irreversibilities perform quite similar normed with the specific mission point fuel exergy consumption but when compared when normed with the mission total average

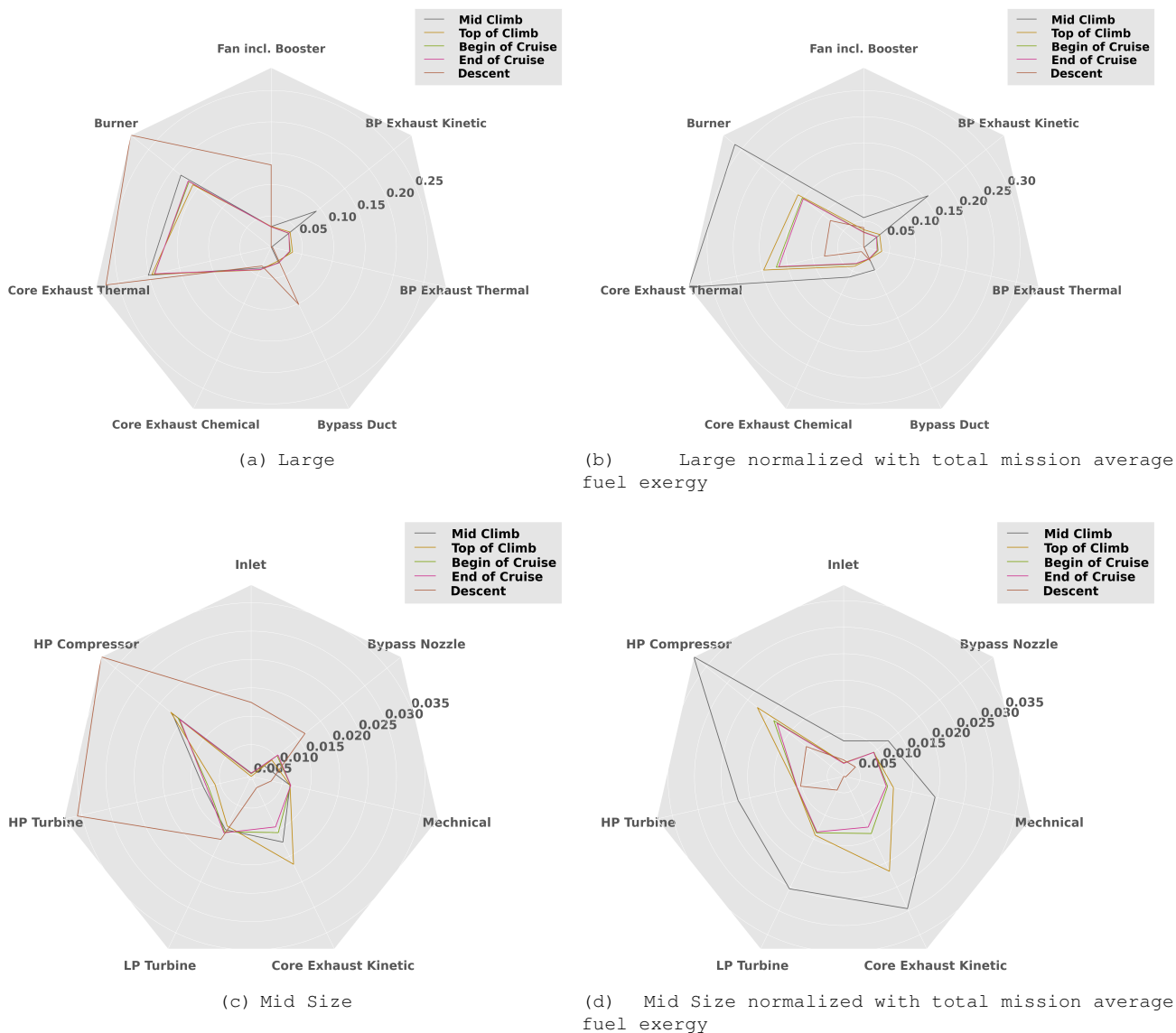


Figure 4: Mission Points - Irreversibilities (All charts scaled after largest included loss).

Table 6: Results of the Total Breakdown of all mission points normalized with consumed exergy

	Mid Climb	Top of Climb	Begin of Cruise	End of Cruise	Descent
Propulsive Power to Aircraft	0.28249	0.31137	0.31185	0.31003	-0.13966
Cabin Supplied Bleed and Power	0.01269	0.01646	0.01795	0.01832	0.04094
Engine System Weight - Potential (stored internal)	0.01533	0.00611	0.00000	0.00000	0.00000
Engine System Weight - Potential (harvested)	0.00000	0.00000	0.00000	0.00000	0.09285
Engine System Weight - Dissipative	0.01368	0.02818	0.03219	0.03307	0.07335
Nacelle drag	0.00764	0.01322	0.01605	0.01652	0.04603
Engine Irreversibility	0.68350	0.63076	0.62196	0.62206	0.88649
Installed Rational Efficiency	0.29518	0.32783	0.32979	0.32835	-0.00586

fuel exergy the points scale with the thrust requirement.

Losses smaller than for the considered large losses, but still significant, are included in the mid size irreversibilities charts in Fig.4(c) and Fig.4(d). The performance of the turbomachinery components in relative terms can be seen to stay relatively constant for the climb and cruise points.

Installed exergy breakdown

Analysis including the installation effect of engine weight and drag brings the control volume from looking at the engine propulsion cycle to the full engine sub system. An exergy breakdown focusing on the engine sub system has been made for the different mission points. The mission total can be seen in Fig.5.

The fuel exergy that goes towards the potential exergy in climb can be seen to be balanced with the harvested potential exergy in descent. This originates from that take off and landing is taking place at the same altitude and that the control volume mass is kept constant throughout the mission.

The simulated mission points are presented in Tab.6 and Fig.6. The cruise points perform at about an installed rational efficiency of about 32.9%, this can be compared to the rational efficiency at 37.8% of the propulsion cycle. The total installed rational efficiency is 29.41% and the engine cycle rational efficiency is 33.46%.

Regarding the descent point, seen from the engine sub system, the negative contribution to the airframe is in terms of the magnitude even larger than for the engine propulsion cycle. The engine sub system also needs to compensate for the dissipative term of the weight equation as well as the nacelle drag.

Discussion and Conclusions

An installed exergy analysis has been applied to a turbofan of a technology level corresponding to year 2020 simulated for the main mission points that constitute a full flight mission. The analysis extends on previous work both by including the effects of weight and drag directly associated with having a propulsion system connected to the aircraft, as well as by featuring detailed studies for the different mission points. The simulation of various mission points help understand the propulsion system performance under the different operating conditions. The developed methodology for the installation effects can also be used to assess the effect of any aircraft component in one common unit. The propulsion system installation effects accounts for about 4% of total work potential in the fuel seen over a full flight mission. Comparing it to the thrust power delivered to the aircraft the ratio becomes one to seven.

A new figure of merit to capture the true performance of a propulsion system has been proposed, namely the *installed rational efficiency*. The measure utilizes the advantages of exergy analysis when relating the propulsion unit supplied useful power to the work potential found in the fuel. The useful power is the power thrust delivered to the aircraft frame as well as the bleed and shaft power supplied to the cabin. The power thrust delivered to the aircraft frame is the thrust supplied by the engine cycle when compensating for the effects of the thrust misalignment, the weight and the drag associated with the propulsion system. The *installed rational efficiency* for the simulated turbofan of a technology level to correspond to year 2020 is 29.41%.

The *installed rational efficiency* term offers a way of assessing the

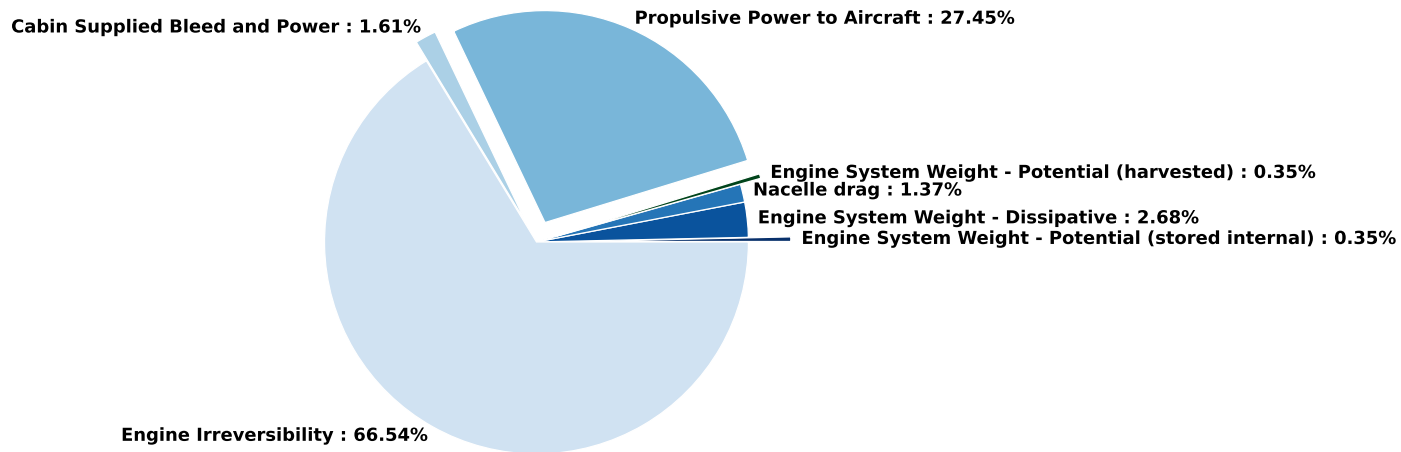


Figure 5: Mission Total - Total installed exergy breakdown

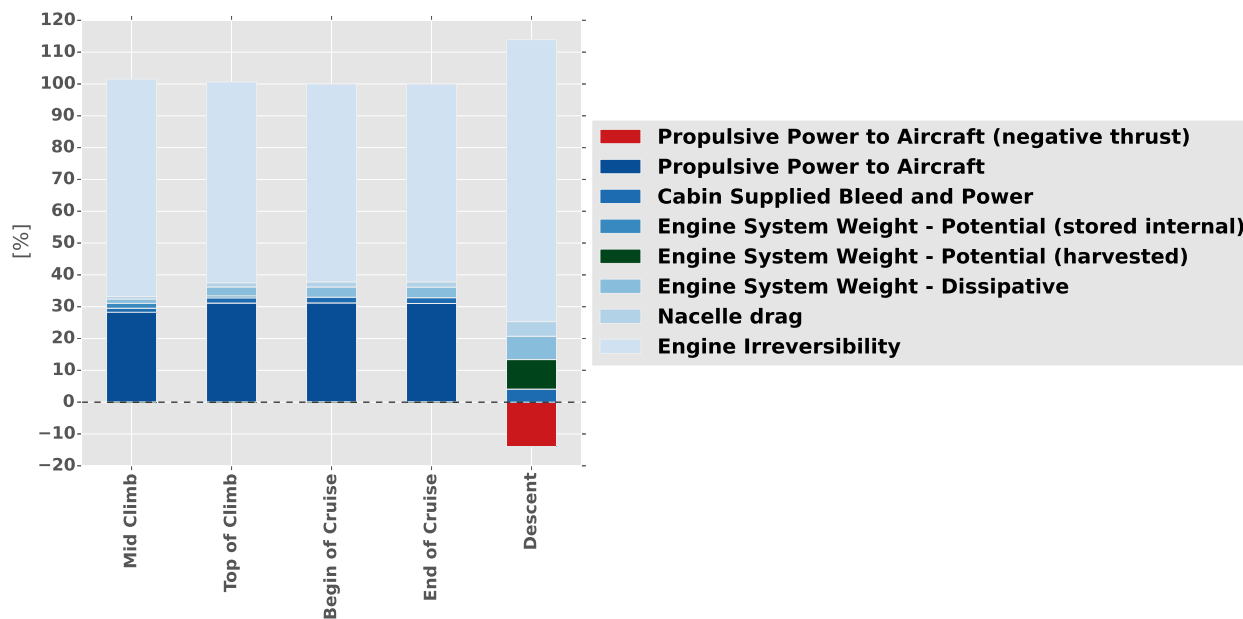


Figure 6: Mission point comparison - Installed exergy breakdown normalized with consumed exergy

propulsion system performance in flight decoupled from the aircraft model. Using an aircraft angle of attack, an aircraft path angle and an aircraft lift over drag coefficient, which are all predefined from an aircraft model, makes this possible. One could use these parameters as applied in this paper to evaluate other engines that are designed for a similar mission type in order to get a comparative measure between different engine configurations.

Acknowledgments

The authors want express their gratitude to Airbus S.A.S. for their support and funding of this work. The authors also want to thank Jonas Lafrenz Schwanemann who during his internship made a significant contribution on the subject of extending the Exergy analysis to take the full effects at aircraft level.

Disclaimer

The data published in this paper were generated solely to be a support to the analysis exercise and are not related to any Airbus product characteristics.

References

- [1] Clarke, J. M., and Horlock, J. H., 1975., ``Availability and propulsion'', *Journal of Mechanical Engineering Science*, 17, p. 223.
- [2] Evans, R. B., 1969., ``A proof that essergy is the only consistent measure of potential work''. PhD thesis, Dartmouth College.
- [3] Brilliant, H. M., 1995. ``Second law analysis of present and future turbine engines''. In Joint Propulsion Conference. AIAA 95-3030.
- [4] Roth, B., McDonald, R., and Mavris, D., 2000. ``A method for thermodynamic work potential analysis of aircraft engines''. In Joint Propulsion Conference, Vol. 38. AIAA2002-3768.
- [5] Grönstedt, T., Irannezhad, M., Xu, L., Thulin, O., and Lundbladh, A., 2014., ``First and second law analysis of future aircraft engines'', *Journal of Engineering For Gas Turbines and Power*, 136.
- [6] Zhao, X., Thulin, O., and Grönstedt, T., 2015. ``First and second law analysis of intercooled turbofan engine''. In ASME Turbo Expo. GT2015-43187.
- [7] Rosen, M. A., 2009., ``Exergy losses for aerospace engines: effect of reference environment on assessment accuracy'', *Exergy, an International Journal*, 6.
- [8] Paulus, D. M. J., and Gaggioli, R. A., 2003., ``The exergy of lift and aircraft exergy flow diagrams'', *International Journal of Thermodynamics*, 6, pp. 149--156.
- [9] Kotas, T. J., 1985. *The Exergy Method of Thermal Plant Analysis*. Butterworths.
- [10] Empresarios Agrupados Internacional. *Proosis - Propulsion Object Oriented Simulation Software*. The VIVACE European Cycle Program.
- [11] Grieb, H., 2004. *Projektierung Von Turboflugtriebwerken*. Birkhauser.
- [12] ESDU International plc, 1981. *Drag of axisymmetric cowls at zero incidence for subsonic Mach numbers*.
- [13] Grönstedt, T., Au, D., Kyprianidis, K., and Ogaji, S., 2009. ``Low pressure system component advancements

and its influence on future turbofan engine emissions''. In Proceedings of ASME Turbo Expo 2009: Power for Land, Sea and Air, GT2009.

- [14] McBride, B. J., and Gordon, S., 1994. *Computer Program for Calculation of Complex Chemical Equilibrium Compositions and Applications*. NASA RP-1311.

Appendix

Exergy Analysis Theory

Without detailed knowledge of the heat transfer process the term needs to be simplified in order to be implemented. In case of the assumption of a perfect gas, the heat transfer integral can be rewritten according to

$$\begin{aligned} -\sum_i \int_0^{Q_i} \frac{T - T_\infty}{T} dQ_i &= -\sum_i \frac{dQ_i}{dT} \int_{T_{i,start}}^{T_{i,end}} \frac{T - T_\infty}{T} dT \\ &= -\sum_i Q_i \left(1 - T_\infty \frac{\ln \left[\frac{T_{i,end}/T_{i,start}}{T_{i,end} - T_{i,start}} \right] \right). \end{aligned} \quad (9)$$

If the temperature is, or can be approximated as constant during the heat transfer, the heat transfer integral in Eq.1 simplifies according to

$$-\sum_i \int \frac{T - T_\infty}{T} dQ_i = -\sum_i Q_i \frac{T_i - T_\infty}{T_i}. \quad (10)$$

This is also consistent when taking the limit of Eq.9.

Regarding the steady flow energy equation, the only difference when moving from the relative to the absolute frame of reference is the change in velocities and the addition of the thrust power term. Therefore, by subtracting the equation from one reference frame to the other, the thrust power can be written as

$$P_T = \left(\sum_i \dot{m}_i \left[\frac{C_i^2}{2} - \frac{V_i^2}{2} \right] \right)_{in} - \left(\sum_i \dot{m}_i \left[\frac{C_i^2}{2} - \frac{V_i^2}{2} \right] \right)_{out}. \quad (11)$$

Using the velocity definition ($c = U - v$), the expression can be simplified to

$$P_T = \frac{U}{2} \left(\left[\sum_i \dot{m}_i (U - 2V_i) \right]_{in} - \left[\sum_i \dot{m}_i (U - 2V_i) \right]_{out} \right). \quad (12)$$

Under the assumption of one inflow and one outflow, the equation can be reduced to

$$P_T = \dot{m}U(V_{out} - V_{in}). \quad (13)$$

If the exhaust nozzle of the engine is choked, then the pressure difference will also contribute to the thrust power. Also, the coefficient of thrust will affect the momentum. The following equations are valid for the nozzle:

$$\begin{aligned} P_{T_{in \rightarrow nozzle}} &= U \left(\left[\sum_i \dot{m}_i c_x V_i \right]_{nozzle} - \left[\sum_i \dot{m}_i V_i \right]_{in} \right) \text{ and} \\ P_{T_{nozzle \rightarrow \infty}} &= \sum_i U A_{nozzle,i} (p_{nozzle,i} - p_\infty). \end{aligned} \quad (14)$$

The specific exergy is calculated by Eq.15. It includes the different forms of exergy that are applicable to an aero engine flying at a constant altitude, i.e. a thermomechanical part (also commonly known as the physical exergy), a kinetic part and a chemical part, i.e.

$$\varepsilon = \underbrace{h - h_\infty - T_\infty(s_{sf} - s_{sf,\infty})}_{\text{Thermomechanical}} + \underbrace{\frac{C^2}{2}}_{\text{Kinetic}} + T_\infty \underbrace{\left(\sum_i \lambda_i R_i \ln \frac{x}{x_{i,\infty}} \right)}_{\text{Chemical}}. \quad (15)$$

Fuel exergy is defined as the maximum work obtainable comparing the state of resting unburned fuel to when the chemical potential of the fuel and the reference environment are in complete equilibrium with each other. Since the chemical part in Eq.16 is derived assuming that the species considered are present in both the system and the reference environment, a different approach must be used. A method for evaluating the exergy of a fuel or for a mixture of species that do not solely consist of species in the reference environment is described in detail by Kotas [9]. One shall note that this is not equal to the LHV value even though it will be quite similar in magnitude. In conformity with the LHV and the HHV calculations, the main contributing energy term in the fuel exergy calculation is based on heat of formation. The entropy for the products after a combustion is much larger than the for the reactants, i.e. heat is captured by the products. The entropy difference

when comparing the products and reactants is included in the chemical fuel exergy term. The difference in enthalpy and entropy comparing the thermomechanical state of the fuel to the ambient conditions is included in the thermomechanical term. The equation is

$$\epsilon_f = \epsilon_{f,\text{phys}} + \epsilon_{f,\text{kin}} + \epsilon_{f,\text{chem}} \quad (16)$$

where the subcomponents are calculated by the following formulas

$$\begin{aligned} \epsilon_{f,\text{ther.mech}} &= \left(\sum_i \beta_i [h_i - h_{ss,i}] - \sum_i \lambda_i [h_{\infty,i} - h_{ss,i}] \right) \\ &\quad - T_{\infty} \left(\sum_i \beta_i [s_i - s_{ss,i}] - \sum_i \lambda_i [s_{\infty,i} - s_{ss,i}] \right), \\ \epsilon_{f,\text{kin}} &= \sum_i \beta_i \frac{C_i^2}{2} \quad \text{and} \\ \epsilon_{f,\text{chem}} &= \sum_i (\beta_i - \lambda_i) * (\Delta h_{f,i}^{\circ} - T_{\infty} \Delta s_{f,i}^{\circ}). \end{aligned}$$

Simulation setup

Fuel exergy is different from the LHV value since it in addition to the difference in chemical enthalpy also includes the change of entropy comparing pre and post combustion as well as the thermomechanical difference between the two states. A way to calculate fuel exergy can be found in Eq.16. This method requires full knowledge of the fuel composition. Jet A is a mixture of various hydrocarbons which therefore becomes less straight forward to model. The engine performance code that was used in this project includes both values of LHV as well as tables to assess the enthalpy difference between two different temperatures. Using both the LHV value and the enthalpy table can account for most of the enthalpy contribution in the fuel exergy equation. The LHV value for the chemical enthalpy contribution and the enthalpy table for the thermomechanical enthalpy contribution of the unburned fuel. Since performance simulations are usually performed at low relative humidities the vapor will not

condense when taking the exhausts to thermodynamical equilibrium with its surroundings. This implies that the LHV shall be used rather than the HHV value in the fuel exergy equation to assess the maximum available work.

Furthermore, combustion of $C_{12}H_{23}$ was assumed to be representative of Jet A in similarity with the NASA developed combustion code Chemical Equilibrium with Applications [14]. This was used to assess the post combustion thermodynamical enthalpy contribution as well as all entropy terms included in the fuel exergy equation. Since the fuel exergy term is larger than the LHV term, using this will lead to that the calculated loss of the combustion chamber is larger than if comparing with the fuel enthalpy difference. The kinetic exergy for the injected fuel was assumed to be zero since it would only have a minor contribution compared to the other terms.

The exergy equations described in Eq.15 cannot handle constituents that solely exist in either the reference or the actual state. Water is a product of the combustion process, an implication of this is that the water content needs to be larger than zero in the reference state. In order to minimize the effect of the non-zero water content but still allow for proper calculations, the ambient relative humidity is set to 1%.